ELSEVIER

Journal of Chromatography A, 969 (2002) 313–322

JOURNAL OF CHROMATOGRAPHY A

www.elsevier.com/locate/chroma

Monitoring and characterization of ink vehicle autoxidation by inverse gas chromatography

C. Castro[a,*], G.M. Dorris[a], C. Daneault[b]

[a]*Pulp and Paper Research Institute of Canada, 570 Boulevard St-Jean, Pointe Claire, Québec, Canada H9R 3J9*

[b]*Centre de Recherche en Pâtes et Papiers, Université du Québec à Trois-Rivières, 3351 Boulevard des Forges, Trois-Rivières, Québec, Canada G9A 5H7*

Abstract

It is now well-established that increased usage of vegetable oils in offset ink formulas aggravates the deinking problems in recycling plants during summer months. The seasonal loss of brightness of recycled paper has been ascribed to increased bonding of oxidatively aged prints to the paper surface. The progress of the oxidative aging of soya bean and linseed oils was followed by inverse gas chromatography. We first report here the rate and extent of vegetable oil oxidation, by measuring the changes in Kovats retention index as a function of the oxidation time. We then characterized the physicochemical changes accompanying the oxidation of vegetable oils from measurements of the partial heat of mixing in the infinite dilution regime.

Keywords: Inks; Inverse gas chromatography; Paper recycling; Vegetable oils; Oxidation

1. Introduction

A large number of North American and European deinking mills experience significant losses of deinked pulp brightness and cleanliness during the summer months [1,2]. It is now well-established that this seasonal phenomenon is the result of the accelerated aging of oil-based inks, induced by exposure of wastepaper to hot conditions during transportation and storage [3–7]. The poor deinkability of aged inks has been ascribed to an oxido-polymerization of the vegetable oils and/or alkyd resins in some inks used in sheet fed offset and into newspapers inks applied on uncoated papers [3,7,8]. In these printing processes, ink dries mainly by penetration of the vehicle in the paper structure. Oil and resin components left on the paper surface with the pigment can react slowly with oxygen to form a three-dimensional polymer network. This conversion of a liquid into a solid film not only increases the cohesiveness of the print but also its degree of bonding to the paper surface [3,7].

Though oxido-polymerization of oil-based inks has long been suspected for the deinking problems in summer months, it is only recently that the various physicochemical changes induced by print oxidation have been studied systematically with model systems. Using thermogravimetry to measure the oxygen uptake, Castro and colleagues [9–11] have established the importance of temperature [10] and of antioxidants [11] to control the aging phenomenon.

In this present work, we complement these results

*Corresponding author. Fax: +1-514-630-4134.

E-mail address: ccastro@paprican.ca (C. Castro).

0021-9673/02/$ – see front matter
PII: S0021-9673(02)00888-9

using an inverse gas chromatographic (IGC) technique that follows the change in polarity of thin films of oil as it reacts in the column with oxygen [12,13]. Because of the trend in the printing industry to increase usage of vegetable oils in coldset offset inks for quality and environmental reasons, we have used here soya bean and linseed oil as representative ink vehicles. Using IGC, kinetics of autoxidation as well as solution thermodynamic parameters of thin films of oils were determined as the oxidation progressed in the chromatographic column.

Vegetable oils consist of a blend of glycerides which are the condensation products of glycerol with one to three fatty acids of variable degrees of unsaturation and with chain lengths of 16–18 carbon atoms. They undergo oxidation reactions by a free radical mechanism [14,15] involving several steps: (1) induction period, during which oxygen reacts slowly with the oil to form hydroperoxides, (2) decomposition of hydroperoxides followed by propagation of the radicals, and (3) termination of the free radical reaction with the formation of cross-links. Several variations of the mechanism of autoxidation of hydrocarbons and lipids have been proposed, but the basic classical kinetic scheme of Bolland [14] still remains the most widely used. If RH represents an organic material with R being a hydrocarbon with a labile hydrogen atom H, the various steps can be represented as:

Initiation:

$$RH + O_2 \xrightarrow{k_{i1}} ROOH \xrightarrow{k_{i2}} \text{free radicals, e.g. } R^{\cdot}, ROO^{\cdot}, RO^{\cdot}, HO^{\cdot} \quad (1)$$

Propagation:

$$R^{\cdot} + O_2 \xrightarrow{k_{p1}} ROO^{\cdot} \quad (2)$$

$$ROO^{\cdot} + RH \xrightarrow{k_{p2}} ROOH + R^{\cdot} \quad (3)$$

Termination:

$$2R^{\cdot} \xrightarrow{k_{t1}} R{-}R \quad (4)$$

$$RO^{\cdot} + R^{\cdot} \xrightarrow{k_{t2}} ROR \quad (5)$$

$$ROO^{\cdot} + R^{\cdot} \xrightarrow{k_{t3}} ROOR \quad (6)$$

where the *k*-values represent the rate constants of the initiation, propagation and termination reactions indicated above. Because of their industrial significance, the chemical reactions by which vegetable oils and their derivatives (e.g. oil modified alkyds) are converted from a liquid to a solid film have received a lot of attention [16–19]. A very large number of variables intervene in the liquid to solid state transformation. It is now well known that the ability of the oil to form the hydroperoxides required to promote the free-radical chain reaction, depends on the number and degree of conjugation of the unsaturated linkages and on the degree of chain branching [16]. Several other parameters such as temperature, oxygen concentration, concentration of antioxidants and catalysts, water content, illumination, film thickness, etc. affect the overall rate of autoxidation [16,17]. In addition to cross-linking reactions, a number of secondary reactions take place as a result of decomposition of hydroperoxides to yield a complex mixture of saturated and unsaturated aldehydes, ketones, esters, hydrocarbons, carbon dioxide and water. The nature of the volatile fraction of the decomposition products has been extensively studied, namely because of the unpleasant odour and/or off-flavours associated with the oxidation of oils used for culinary [12,20,21] and painting applications [22].

Several methods can be used to follow the course of the overall oxidation process, but in bulk liquids, the rates of oxygen gas uptake or of peroxide formation and decomposition are the most widely used since they provide the most direct quantitative results [15,21]. To study oil oxidation of thin films, it is more convenient to probe physicochemical changes such as polarity, carbonyl and hydroxyl content, that take place with oxidation time. It has been shown in numerous studies that the polarity changes can be conveniently monitored by IGC [12,23–25], using for example changes in Kovats retention index [26] as a function of oxidation time. IGC has also been used to evaluate the bulk fundamental thermodynamic parameters as the oxidation of vegetable oils progressed in the chromatographic column.

2. Experimental

2.1. Materials

Soya bean oil and linseed oil (no additives) were both commercial products obtained from Natural Health, Laprairie, Canada. The composition of linseed oil is typically 13–37% oleic acid (18:1), 5–23% linoleic acid (18:2) and 26–58% linolenic acid (18:3). Soya bean oil has a fatty acid composition of 24–31% oleic (18:1), 49–51% linoleic (18:2) and 2–10% linolenic (18:3) [27]. The following solutes were used as probe: acetone, *n*-butanol, diethyl ether, dichloromethane, trichloromethane, tetrachloromethane, benzene, toluene, *n*-pentane, *n*-hexane, *n*-heptane, *n*-octane, *n*-nonane and *n*-decane. All solutes were reagent-grade obtained from Sigma–Aldrich Canada, Oakville, Canada, and were injected without further purification. Chromosorb G (60–80 mesh) from Chromatographic Specialties, Brockville, Canada, was used as inert solid support. Prepurified gases were obtained from Praxair, Trois-Rivières, Canada.

2.2. Apparatus

IGC measurements were carried out on a Varian 3700 gas chromatograph from Varian Canada, Montreal, Canada, equipped with a flame ionization detector. Prepurified gases were used as carrier or oxidizing gases. Methane was used as the non-interactive marker to estimate the dead volume in the column. The columns (1.8 m × 0.63 cm) were packed with 10% mixtures of vegetable oils and Chromosorb G. The packing was prepared by dissolution of oil in dichloromethane followed by slow solvent evaporation in a rotary evaporator. Preliminary work [9] had indicated that at 10% coating and above, bulk sorption was the sole mechanism responsible for the retention of the various solutes studied here.

The following operating conditions were employed: injector temperature 130 °C, detector temperature 160 °C, carrier gas and oxidizing gas at a flow-rate of 30 ml/min.

2.3. Retention measurements and oil oxidation

The method of Evans [28] was used to make the retention measurements on unoxidized and oxidized oil substrates. The columns with freshly prepared oil coatings were first purged for 2 h at room temperature with a flow of nitrogen. Then the system was brought to the target column temperature and allowed to stabilize for 4 h, under a nitrogen flow. The various solutes were then injected at infinite dilution into the column. To initiate the oxidation, oxygen was mixed with nitrogen at a pre-set ratio. At regular intervals, the flow of oxygen was interrupted and the retention measurements were made on the oil substrates using nitrogen as the gas carrier.

2.4. Data reduction

The oxidation of the two vegetable oils was monitored at various temperatures from the changes in the adjusted retention times, used to estimate Kovats' retention index, *I*, by:

$$I = 100N + 100n \cdot \left[\frac{log\, R_X - log\, R_N}{\log R_{N+n} - log\, R_N} \right] \qquad (7)$$

where R_X is the adjusted retention time of a polar probe, and R_N and R_{N+n} are the adjusted retention times of *n*-alkanes containing N and $N+n$ carbon atoms, respectively. Adjusted retention times were measured between individual peak maxima and that of methane. Hence by following the changes in I with time allowed us to monitor the progress of oil oxidation. We have used many probes to obtain different Kovats' indices [9]; however, we will report only the data for *n*-butanol because this probe was the most sensitive one to follow oil oxidation. Kinetics of oil oxidation was determined from changes in Kovats' indices with oxidation time and temperature.

To gain some insight on the changes in polarity of the oil substrates as the oil oxidized, we have also determined a number of bulk thermodynamic parameters from the specific retention volume, Vg^{o} given by Eq. (8) [13].

$$Vg^{o} = \frac{273.16\,(F)(t_R - t_M) \cdot \left(\frac{3}{2} \left[\frac{(P_{in}/P_o)^2 - 1}{(P_{in}/P_o)^3 - 1} \right] \right) \cdot \left(\frac{760}{P_o} \right) \cdot \left(1 - \frac{P_w}{P_o} \right)}{Tw} \qquad (8)$$

where F is the flow-rate at ambient conditions, t_R

and t_M are the retention times of the probes and of methane, P_{in}, P_o and P_w are, respectively the inlet, outlet and the water vapour pressures in the bubble flow meter; T is the column temperature and w is the weight of the stationary phase (i.e. oil). Values of Vg^o at infinite dilution were used to calculate the thermodynamic solution parameters for the solubilization of a vapour (the solute) with a liquid (the stationary phase). The weight fraction-based activity coefficient, Ω^∞, was determined using commonly used expression [13,29]:

$$\Omega^\infty = \frac{273.16R}{Vg^o M p^o \exp\left[\frac{B_{11}-V}{RT}p^o\right]} \quad (9)$$

where the superscript ∞ refers to infinite dilution of the probe in the oil, R is the gas constant, M is the molecular mass of the solute, p^o is saturated vapour pressure of the solute at a temperature T, B_{11} is the second virial coefficient of the solute estimated from Lennard-Jones state equation [30] and V is the molar volume of the solute. The enthalpy for mixing, ΔH_m^∞, was obtained from the following expression [13]:

$$\Delta H_m^\infty = R \cdot \frac{\partial \ln \Omega^\infty}{\partial(1/T)} \quad (10)$$

3. Results and discussion

3.1. Monitoring the progress of the oxidative aging

Fig. 1 shows how the retention index of two common vegetable oils, namely soya bean and linseed oil, change with time upon exposure to dry air (20% O_2, 80% N_2 and 0% RH) at 25 °C. The IGC technique obviously follows well the three stages of autoxidation: induction, propagation and termination, as already reported by Evans and Newton [23,24]. In our analysis of these sigmoidal shape curves, we use two characteristic features [10]; the induction time (t_{ind}) and the maximal oxidation rate (R_{mox}). Determination of these parameters is illustrated in Fig. 1.

As demonstrated in deinking studies [8,10,11], the induction stage is the most important step to control because it represents the demarcation between trouble-free and troublesome deinking [8]. At 25 °C, the induction stage lasts over 60 days for soya bean oil, but only 10–12 days for linseed oil. The lower reactivity of soya bean oil compared to linseed oil is attributed to its higher oleic acid content because oleic acid has a significantly lesser tendency to oxidative polymerization than linoleic and linolenic acid segments.

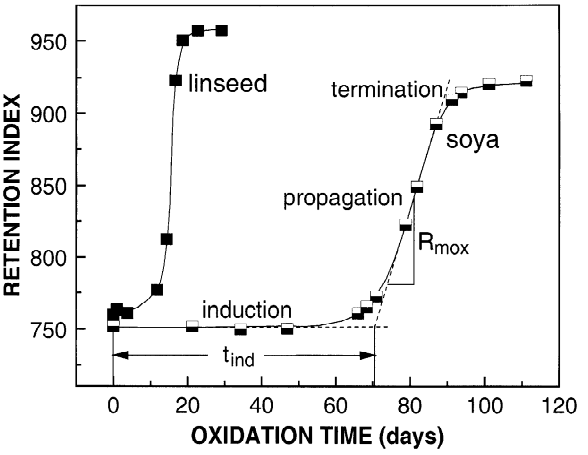

Fig. 1. Natural autoxidation of linseed and soya bean oil, 25 °C and 20% oxygen concentration.

In the induction stage, oxygen reacts with the oil slowly to form hydroperoxides (reaction 1), and the small and progressive oxygen uptake leads to very little change in the retention index. Once the concentration of hydroperoxides has reached a critical value, a change in initiation mechanism takes place. Beyond this time, the mechanism of formation of free radicals changes from hydroperoxide monomolecular decomposition kinetics to bimolecular decomposition [21]. As a result of this change of mode, free radicals are generated at an increasing rate, which then triggers the propagation stage. In the second stage, oxygen reacts preferentially with the free radicals (reaction 2). As this free radical reaction is much faster than that of the formation of hydroperoxides, oils absorb oxygen at an increasing rate. Moreover, the oxygenated free radicals formed by reaction 2 can react with the oil substrate to produce new free radicals susceptible to oxidation (reaction 3). As oxygen is fixed by the oil substrate, the retention index increases. The demarcation between the induction and the propagation stage is rather arbitrary. To identify the end of induction and

the onset of fast oxidation, the linear region of the propagation stage was extrapolated to the retention index prior to the oxidation. After a linear increase in the oxygen uptake during the propagation stage, there is a decrease in the oxidation rate due to the depletion of the available oxidation sites in the oil. During this third stage (i.e. termination), free radicals react preferentially with themselves to form cross-links (reactions 4–6). Fig. 1 also shows that the total gain in retention index is ~160 units for soya bean oil and ~200 units for linseed oil.

During propagation, compounds of different chemical nature are formed (i.e. aldehyde, alcohol, ketone, ether). The polarity and hence the retention index will then depend on the quantity of oxygen absorbed but also on the type of groups formed. Despite the complexity of the reaction pathways, our work [9–11] and the work of others [12,21,23] show that in the propagation stage, autoxidation of oil reaches a steady-state characterized by a constant rate of oxygen uptake. The fact that this steady-state is also observable by IGC as a linear increase in retention index (Fig. 1), suggests that IGC data can yield useful information on the kinetics of this stage.

It can be therefore ascertained that this IGC method can yield reliable kinetic data in the induction period, which is the most important one for the control and prevention of ink aging. However, after the induction step, the heterogeneous chemical nature of the oxygenated compounds formed, complicates the relation between retention index and oxygen absorption. Despite this shortcoming, the analysis of the maximal oxidation rate in the next section shows that this IGC parameter can be used to analyze the kinetics of the propagation stage.

3.2. Effect of temperature and oxygen concentration

To establish the relative importance of temperature and oxygen concentration in the gas phase on the autoxidation process, kinetic data obtained from t_{ind} and R_{mox} measurements were fitted to a statistical model using a step-wise regression algorithm. The data were fitted to an exponential model of the form:

$$t_{ind} \text{ or } R_{mox} = \exp(b_0 + b_1[O_2] + b_2T + b_3T^2) \quad (11)$$

Table 1
Regression model coefficients and R^2 for t_{ind} and R_{mox} of linseed and soya bean oils

Reg. coeff.	Linseed oil		Soya bean oil	
	t_{ind}	R_{mox}	t_{ind}	R_{mox}
b_0	7.8541	−3.1068	9.3620	−5.5546
b_1		0.0586		0.0582
b_2	−0.0814	0.1122	−0.0814	−0.1481
b_3		−0.0004		−0.0006
R^2	0.99	0.97	0.99	0.99

where t_{ind} is expressed in h and R_{mox} in 1/h, $[O_2]$ is the oxygen concentration in % volume and T is the temperature in °C. The regression coefficients which were found to be significant at the 95% level of confidence and the correlation coefficients, R^2 for the soya bean and linseed oil data are presented in Table 1. Temperature (linear effect) is found to be the only regressor affecting the values of induction times. On the other hand, the maximal oxidation rate is affected by both the oxygen concentration and by the temperature. Analysis of variance for significance indicated that temperature had the largest effect on t_{ind} and R_{mox}.

In Fig. 2, the fit of the model to the experimental induction times for linseed and soya bean oils is presented. The quality of the fit suggests the adequacy of the logarithmic model. Within the range studied, induction time is independent of oxygen concentration and is solely a function of temperature.

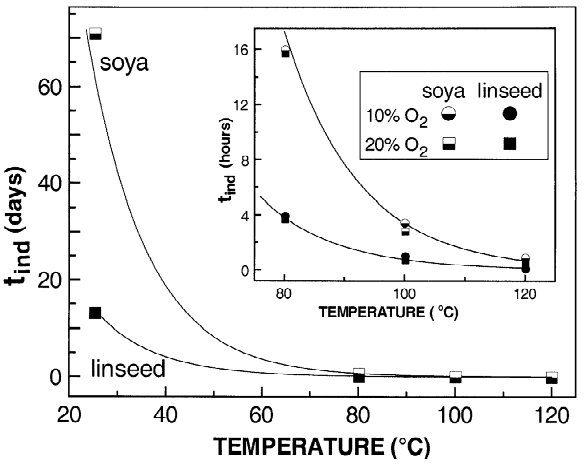

Fig. 2. Induction times for linseed and soya bean oils. Symbols (experimental results); lines (values predicted from model).

This result indicates that in the initiation stage, the concentration at which oxygen becomes rate-limiting must be well below 10% (v/v) (or 10 kPa). At lower temperatures (25–80 °C), the induction time is very sensitive to a small change in temperature whereas above 100 °C, the induction time becomes barely detectable. It has been proposed that formation of the first hydroperoxides required to initiate the free radical chain reaction requires the production of singlet-state O_2 via sensitizers which are always present in vegetable oils [31]. The large effect of temperature on the reduction of the induction time may possibly involve the enhanced formation of singlet-state O_2 at higher temperatures. Fig. 2 also shows that the induction times for linseed oil are shorter than for soya bean oil. These results are consistent with those made from other types of measurements such as viscosity on the bulk polymerization of vegetable oils [32] or the mass gain monitored by a thermogravimetry method [10].

Figs. 3 and 4 show that the fit of the exponential model to the oxidation data for linseed and soya bean oil, respectively, is also reasonably good. These figures clearly show that an increase in temperature always increases R_{mox}. Above 100 °C, the slope of the curve decreases probably due to the elution from the column of degradation products [10]. Unlike the t_{ind}, R_{mox} is dependent on the oxygen concentration. At all temperatures, a decrease in the oxygen concentration reduces R_{mox}. In the autoxidation scheme described previously, decreasing the oxygen concentration reduces the overall rate of oxidation only when the reaction between oxygen and the free radical $R^{\cdot}$ (reaction 2) is not much faster than the hydroperoxide radical reaction with the fatty acid ester moiety, RH (reaction 3). As only reaction 3 of the propagation step is greatly influenced by temperature, the rate-limiting oxygen concentration should increase with increasing temperature [12]. This oxygen concentration dependence is observed in Figs. 3 and 4 by the larger R_{mox} differences at higher temperature. Past the induction stage, linseed oil oxidizes only slightly faster than soya bean oil, but the extent of oxygen uptake for linseed oil seems to be larger as indicated by the higher value of the retention index.

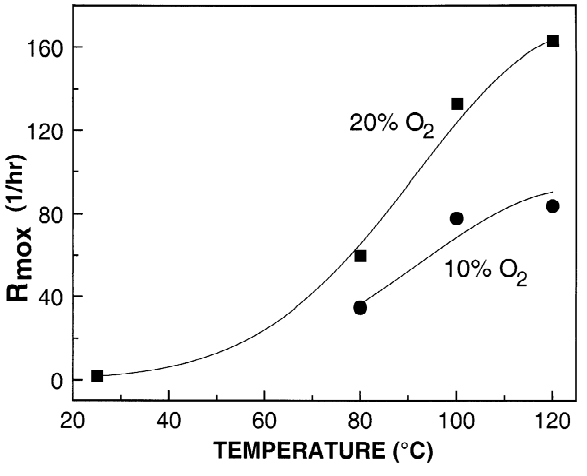

Fig. 3. Maximal oxidation rates for linseed oil. Symbols (experimental results); lines (values predicted from model).

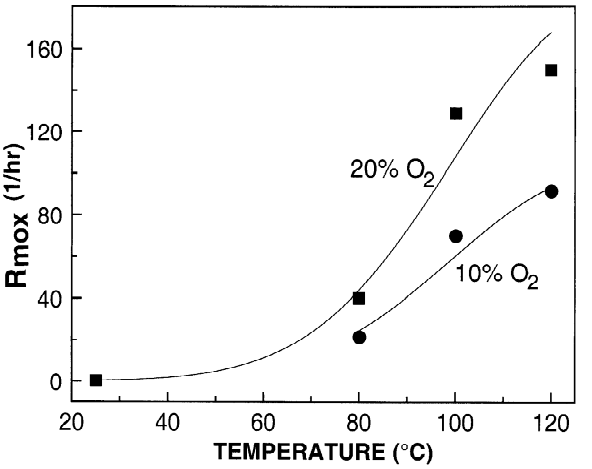

Fig. 4. Maximal oxidation rates for soya bean oil. Symbols (experimental results); lines (values predicted from model).

3.3. Activation energies

According to general kinetics theory, the activation energy can be determined by the classical Arrhenius equation:

$$k = Ae^{-E_a/RT} \tag{12}$$

where k is the rate constant, A is a constant, R the gas constant and T the temperature. Lipid oxidation can be broken down into a number of elementary

reactions, each with its own activation energy. According to Labuza [21], the end of initiation is characterized by a critical hydroperoxide concentration [$ROOH_{cr}$] of about 0.5–1% (molar basis). The rate for the induction period, R_{ox}, follows a rate law of the form:

$$R_{ox} = \frac{-\mathrm{d}[O_2]}{\mathrm{d}t} = b \cdot \frac{1}{t_{ind}} \cdot [ROOH_{cr}]^{1/2} \quad (13)$$

where $[O_2]$ is the concentration of oxygen absorbed and b a proportionality constant. As t_{ind} is inversely proportional to k, a plot of ln $(1/t_{ind})$ versus $1/T$ gives a straight line with E_a/R as the slope (Fig. 5). After the induction stage, the oxidation rate is governed by the equilibrium hydroperoxide concentration, as shown by Eq. (14) [21]. This steady-state concentration remains constant for a good part of the propagation stage. The oxidation rate being unchanged, the overall system behaves as a zero-order reaction ($R_{ox} = k$). Under these conditions, a plot of ln (R_{mox}) against $1/T$ gives a straight line with a slope of E_a/R.

$$R_{ox} = R_{mox} = \frac{-\mathrm{d}[O_2]}{\mathrm{d}t} = k[ROOH_{eq}] \quad (14)$$

Table 2 presents calculated values of activation energy for the induction and the propagation stages. Induction activation energies of the two oils are not significantly different. The high value of 79 kJ/mol is in good agreement with that of pure lipids reported

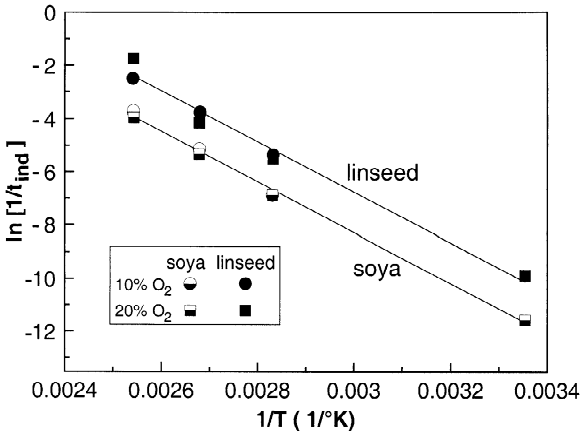

Fig. 5. Activation energy determination for the induction period.

Table 2
Activation energies for the linseed and soya bean oxidation

Oil	E_a (kJ/mol)	
	Induction	Post-induction
Linseed	78.9±5.6	53.5±2.2
Soya	79.0±2.2	73.2±2.1

(~84 kJ/mol) [21]. Hence the temperature dependence is nearly the same for both oils, even though the induction times for linseed oil are much shorter than for soya bean oil. These results suggest that the initiation mechanism for both oils is similar, though the length of the induction period is affected by the number of reactive sites in the oil.

Table 2 also shows that the values of activation energy of both oils are lower in the propagation stage than in the induction stage, but that the energy barrier for oxidation is higher for the soya bean oil than linseed oil due to a fewer number of reactive sites. This kinetic study reveals that the initiation reactions in the induction period are rate-determining. A small change in temperature, particularly in the temperature range pertaining to natural aging, reduces greatly the induction period. Because the formation of hydroperoxides by fixation of oxygen in the oil proceeds very slowly in the initiation stage, only low concentrations of oxygen in the gas phase are required. It is likely that the threshold concentration at which oxygen concentration becomes rate-limiting is already exceeded during the transportation and storage of old newspapers. Hence, the oxidative aging of the print starts right after printing and proceeds without interruption until the old paper is finally repulped. The relationship between the autoxidation of vegetable oil films and the deinkability of offset-printed newspapers has been demonstrated recently [8].

3.4. Monitoring the changes in chemical interaction

In the previous section, IGC was shown to be a useful tool for following the kinetics of autoxidation of vegetable oils used in offset inks. Observations made at low temperature in particular, explain well why deinking of vegetable oil-based inks is more difficult during the summer months. These findings

indicate that it is possible to take preventive measures during waste paper transportation and storage to avoid having a large proportion of the oil vehicles in the propagation stage of the autoxidation process [8]. Once this stage is reached, the enhanced interaction between the print and the paper surface leads to a more incomplete detachment of the print during repulping and hence to a more grayish and dirtier pulp.

To find better chemical strategies than the conventional ones to enhance the detachment of oxidized print, we have used IGC to give some insight on the changes in interaction between soya bean and linseed oil and various types of gaseous probes, before and after oxidation. Using IGC, King and List [13] have already reported thermodynamic solution parameters of unoxidized soya bean oil. A similar approach was used here. From the specific retention volumes of various probes measured at different temperatures, a number of thermodynamic and interaction parameters in the infinite dilution regime were determined [9], using well-known approaches [29,33]. Since many of the determined parameters provide similar information based in the concept ''like dissolves like'', for conciseness, only the partial heats of mixing will be reported here. As shown previously, ΔH_m^∞ is calculated from the temperature dependence of the activity coefficient (Eq. (10)).

3.5. Heat of mixing

In general, high negative values of heats of mixing are indicative of a strong solute–oil interaction and hence that this solute has a good solubilizing power for the oil substrate. The resultant ΔH_m^∞ values are presented in Table 3 for four classes of solutes. The error in ΔH_m^∞ values determined from the standard deviation of the slopes is less than 3% in all the cases. For comparison, values reported by King and List with a soya bean stationary phase, are also reported in Table 3.

Except *n*-butanol, all solutes have negative values of ΔH_m^∞, suggesting that the enthalpic component of the solution promotes dissolution. These values are however not large and, as suggested by King and List [13], this may indicate that the free energy of

Table 3
Heats of mixing for different solutes, before and after linseed and soya bean oil oxidation

Oil oxidation solutes	ΔH_m^∞ (kJ/mol)				
	Linseed oil		Soya bean oil		
	Before	After	Before		After
			This work	Ref. [13]	
Oxygenated					
n-Butanol	6.47	−1.38	6.84	11.51	−0.68
Acetone	−1.05	−5.13	−1.06	2.64	−4.04
Diethyl ether	−4.33	−4.67	−3.95		−4.09
Chlorinated					
Dichloromethane	−5.13	−7.46	−4.74		−5.75
Trichloromethane	−6.70	−8.21	−5.94		−7.22
Tetrachloromethane	−4.82	−5.95	−4.49	−0.71	−4.78
Aromatic					
Benzene	−3.22	−4.38	−2.97	3.34	−3.55
Toluene	−3.59	−4.39	−3.30	2.42	−3.60
Alkanes					
n-Pentane	−3.82	−3.01	−3.69		−2.96
n-Hexane	−3.14	−2.57	−3.10	0.58	−2.13
n-Heptane	−2.74	−1.69	−2.60	1.46	−1.49
n-Octane	−2.43	−1.37	−2.29	6.48	−0.93

solution is dominated by the entropy of mixing. As the two oils oxidize, the general tendency for all the probes is an increase in ΔH_m^∞, though the magnitude of the increase is greater for the oxygenated solutes. Hence, fixation of oxygen in the triglycerides enhances their interaction with probes capable of interacting by hydrogen bonding. Chlorinated probes, which are electron-acceptors and hence acidic probes, present the highest negative values of ΔH_m^∞, both before and after oxidation. Moreover the values of ΔH_m^∞ increase upon oil oxidation suggesting that oxidation increases the basic character of vegetable oils. On the other hand, *n*-alkanes, which interact with oil by dispersion forces only, tend to have slightly reduced values of heat of mixing as the oils oxidize.

Comparison of our IGC determinations of ΔH_m^∞ with those of King and List [13] for the unoxidized soya bean system reveals significant differences. Qualitatively the trends between different classes of solutes are similar but our values tend to be generally lower. These differences are probably due to the difference in the source and treatment of the soya bean oils used in the two studies.

The importance of the source of oil combined with the unavoidable loss of weight of the stationary phase, especially after an exposure to an oxygen atmosphere, therefore limit the accuracy of the determination of thermodynamic parameters. Despite these limitations, IGC remains useful to understand the changes in interaction, brought about by in-situ fixation of oxygen in the stationary phase.

4. Conclusions

IGC has been used here as a tool to understand better the adverse role of the autoxidation process on the deinkability of newspaper printed with vegetable oil-based inks. Use of IGC allowed the monitoring of the aging process of thin films of vegetable oils under natural and accelerated aging conditions. Kinetics parameters obtained for the induction and propagation phase of the autoxidation process provided useful practical information on deinkability not easy accessible by other techniques. Changes in interaction between various type of probes and the oil substrate both before and after oxidation helped to understand why detachment of the print from cellulosic fibres is so difficult during summer months and also how this detachment could be enhanced using deinking chemicals with a more acidic character.

5. Nomenclature

Ω^∞	weight fraction-based activity coefficient at infinite dilution
A	constant from Arrhenius equation
B_{11}	second virial coefficient of the solute, ml/mol
b	proportionality constant
b_0–b_3	regression coefficients
E_a	activation energy, kJ/mol
F	flow-rate at ambient conditions, ml/min
ΔH_m^∞	enthalpy for mixing at infinite dilution, kJ/mol
I	Kovats' retention index
k	rate constant
k_i	initiation rate constant
k_p	propagation rate constant
k_t	termination rate constant
M	molecular mass of the solute, g/mol
N	number of carbon atoms of alkane detected before the probe
$N+n$	number of carbon atoms of alkane detected after the probe
$[O_2]$	oxygen concentration in the gas, % v/v
P_{in}	inlet pressure, mmHg (1 mmHg = 133.322 Pa)
P_o	outlet pressure, mmHg
P_w	water vapor pressure in the bubble flow meter, mmHg
p^o	saturated vapour pressure of the solute, mmHg
R	gas constant, 6.236×10^4 ml mmHg K^{-1} mol^{-1}
R^2	correlation coefficient
R_{mox}	rate of maximal oxidation, 1/h
R_N	adjusted retention time of alkane containing N carbons atoms, min
R_{N+n}	adjusted retention time of alkane containing $N+n$ carbons atoms, min

$[ROOH_{eq}]$	equilibrium hydroperoxide concentration, mol/l
$[ROOH_{cr}]$	critical hydroperoxide concentration, mol/l
R_X	adjusted retention time of polar probe, min
T	column temperature, K
t_{ind}	induction time, days or h
t_M	retention time of methane, min
t_R	retention time of probes, min
V	molar volume of the solute, ml/mol
Vg^o	specific retention volume, ml/g
w	weight of the stationary phase, g

References

[1] R.D. Haynes, A. Hestner, Prog. Pap. Recycling 10 (2001) 35.
[2] R.D. Haynes, Tappi J. 83 (2000) 56.
[3] H. Settler, Wochenbl. Papierfabr. 107 (1979) 866.
[4] L.O. Larsson, H. Busk, Wochenbl. Papierfabr. 113 (1985) 573.
[5] E. Frank, Wochenbl. Papierfabr. 118 (1991) 819.
[6] J. Rosinski, Prog. Pap. Recycl. 4 (1995) 55.
[7] J. Blechsmidt, A. Knittel, A.M. Strunz, Wochenbl. Papierfabr. 121 (1993) 783.
[8] G.M. Dorris, N. Pagé, Prog. Pap. Recycling, 9 (2000) 14, 21.
[9] C. Castro, Ph.D. Thesis, UQTR (1998).
[10] C. Castro, C. Daneault, G.M. Dorris, J. Pulp Pap. Sci. 22 (1996) J365.
[11] C. Castro, C. Daneault, G.M. Dorris, Pulp Pap. Can. 100 (1999) 54.
[12] R. Bird, M. Evans, Chromatographia 19 (1984) 180.
[13] J. King, G. List, J. Am. Oil Chem. Soc. 67 (1990) 424.
[14] J.L. Bolland, Proc. R. Soc. A186 (1946) 218.
[15] L. Bateman, Q. Rev. 8 (1954) 147.
[16] H. Wexler, Chem. Rev. 64 (1964) 591.
[17] N. Hartshor, J. Coatings Technol. 54 (1982) 53.
[18] N. Falla, J. Coatings Technol. 64 (1992) 55.
[19] N. Delahaye, J.M. Saiter, M. Liziard, L. Podgorski, J. Coatings Technol. 67 (1995) 67.
[20] J.A.F. Faria, J. Am. Oil Chem. Soc. 60 (1983) 1.
[21] T.P. Labuza, CRC Crit. Rev. Food Technol. 2 (1971) 355.
[22] R.A. Hancock, N.J. Leeves, P.F. Nicks, Prog. Org. Coat. 17 (1989) 321.
[23] M.B. Evans, R. Newton, Chromatographia 9 (1976) 561.
[24] M.B. Evans, R. Newton, Chromatographia 11 (1978) 311.
[25] A. Sen, R. Kumar, Lubrication Eng. 47 (1991) 211.
[26] E. Kovats, Helv. Chim. Acta 41 (1958) 1915.
[27] B. Fuchs, U. Lindqvist, E. Walström, in: Proceedings of the Technical Association of the Graphics Arts, Rochester, NY, 1991, p. 433.
[28] M.B. Evans, Chromatographia 36 (1993) 241.
[29] P. Munk, Chem. Anal. 113 (1991) 150.
[30] A.F.M. Barton, CRC Handbook of Solubility Parameters and Other Cohesion Parameters, CRC Press, 1st ed. (1983).
[31] H.R. Rawls, P.J. Van Santen, J. Am. Oil Chem. Soc. 47 (1970) 121.
[32] P.S. Hess, G.A. O'Hare, Ind. Eng. Chem. 42 (1950) 1424.
[33] D.G. Gray, Prog. Polym. Sci. 5 (1977) 1.